Water Air Soil Pollut (2014) 225:2101
DOI 10.1007/s11270-014-2101-z

Removal of Rhodamine 6G from Aqueous Effluents by Electrocoagulation in a Batch Reactor: Assessment of Operational Parameters and Process Mechanism

Laura Zaleschi · Marius Sebastian Secula · Carmen Teodosiu · Corneliu Sergiu Stan · Igor Cretescu

Received: 1 May 2014 / Accepted: 24 July 2014 / Published online: 8 August 2014

Abstract The aim of the present study is to investigate the effects of operating conditions and establish the mechanism of xanthene dye removal from aqueous solutions by electrocoagulation (EC) using a batch-stirred cell operated under galvanostatic regime. The influence of the operating parameters such as: initial pH and dye concentration, electrolysis time, current density, electrode configuration, and electrical current type on the EC performances was investigated. EC tests were performed at current density values ranging from 45 to 109 A/m, initial dye concentrations ranged between 0.1 and 1 g/L, and initial pH values adjusted in the range from 3 to 9. The effects of several electrode configurations (aluminum–aluminum, mild steel–mild steel, and aluminum–mild steel) and current regimes (direct current and alternating pulsed current) on the removal efficiency and energy and material consumption are also discussed. Total organic carbon (TOC) analysis, UV–vis spectroscopy, Fourier transform infrared spectroscopy (FTIR), and cyclic voltammetry (CV) were employed in order to elucidate the decolorization mechanism of Rhodamine 6G (R6G) dye by EC in aqueous solutions. With this aim in view, chemical coagulation tests were also carried out. The best performance was obtained when the EC process was conducted with iron-based electrode configuration in alternative pulse current (APC) mode. It was found that the removal of R6G is due to the co-precipitation of polymeric iron flocs with the phenyl-xanthene radicals remained in the bulk solution after the demethylation and deamination processes. Furthermore, the flocs are separated by flotation with the support of the molecular hydrogen generated at the cathode (in particular at relatively high values of current density) or by sedimentation.

Keywords Electrocoagulation · Decolorization · Rhodamine 6G · Mechanism · Energy consumption

L. Zaleschi · C. Teodosiu (✉) · I. Cretescu
Department of Environmental Engineering and Management, Faculty of Chemical Engineering and Environmental Protection, "Gheorghe Asachi" Technical University of Iasi (TUIASI), 73 Prof. Dr. Doc. Dimitrie Mangeron Street, 700050 Iasi, Romania
e-mail: cteo@ch.tuiasi.ro

M. S. Secula · C. S. Stan
Department of Chemical Engineering, Faculty of Chemical Engineering and Environmental Protection, "Gheorghe Asachi" Technical University of Iasi (TUIASI), 73 Prof. Dr. Doc. Dimitrie Mangeron Street, 700050 Iasi, Romania

1 Introduction

Dye-containing effluents raise serious environmental issues and public health concerns if these are insufficiently treated before their discharge in rivers/seas (Ansari et al. 2011; Khan et al. 2011; Tiwari et al. 2011; Xia et al. 2012). Their release in water bodies obstructs the light penetration, leading to the inhibition of the photosynthesis-based biological processes (Tang et al. 2012). These effluents may also contain chemicals that are toxic, carcinogenic, mutagenic, or teratogenic for aquatic ecosystems and humans.

Therefore, it is important to apply an adequate treatment on dye effluents for the color removal before their discharge (Aquino et al. 2013; Căilean et al. 2013; Khalfaoui et al. 2012; Khan et al. 2011). Due to the consumption of large volumes of water, textile dyeing industry is one of the most important generators of dye-containing wastewater (Ansari et al. 2011; Bayramoglu et al. 2013; Căilean et al. 2009). Jekel (1997) reported that each ton of produced fabric consumes 20–350 m^3 of water (Jekel 1997). The interest in environmentally friendly wet-processing textile techniques has increased in recent years and water recycling alternatives are considered for implementation (Babu et al. 2007; Wei et al. 2012).

Rhodamine 6G (Basic Red 1) is a monocationic xanthene dye (Halterman et al. 2010) being used on a large scale in the textile industry to dye silk, cotton, wool, fibers, paper, leather, plastics, and as tracing agent in water pollution studies (Jhonsi et al. 2009; Martinez-Huitle and Brillas 2009). Xanthene dyes are based on fluorescein- and Rhodamine-like structures with an intensive fluorescence. They are used like molecular probes for bioanalytical application and for cellular imaging, in laser surgery, as an insecticide and drug screening (Halterman et al. 2010; Khalfaoui et al. 2012; Tang et al. 2012).

Hazardous xanthene dye, R6G, has been proven to induce chromosomal aberrations in cultured CHO (Chinese hamster ovary) cells and has incidence of keratoacanthomas of the skin. The carcinogenicity, reproductive and developmental toxicity, neurotoxicity, and chronic toxicity to humans and animals have been experimentally proven (Ingale et al. 2012; Khalfaoui et al. 2012).

Various conventional or advanced treatment processes have been used to eliminate or separate textile dye from the wastewaters like adsorption on different materials, coagulation, flocculation, photo-oxidation, ozonation, ultrasonication (Căilean and Teodosiu 2012), electrooxidation (Bebeselea et al. 2008; Vlaicu et al. 2011), and electrocoagulation (Merzouk et al. 2011; Parsa et al. 2011; Secula et al. 2011; Venkatraman et al. 2012).

R6G dye has a high molecular mass which makes it difficult to separate by adsorption. Other conventional methods, such as chemical coagulation, are not effective especially due to the very good solubility of R6G in water. Our tests showed that the conventional coagulation is ineffective in separating R6G from aqueous solutions. R6G dye is known for its bio-refractory and outstanding photostability (Zollinger 2003).

Electrocoagulation processes might represent a simple, reliable, and efficient method for wastewater treatment, the chemicals needed being minimal (generally not more than 60 ppm of NaCl in order to ensure the necessary electrical conductivity) and at the same time the treatment costs being lower than in case of chemical coagulation. Bayramoglu et al. (2007) performed an economical assessment showing that the operation cost for chemical coagulation was 3.2 times more expensive than that of electrocoagulation process (Bayramoglu et al. 2007). Also, the sludge quantity was reduced in comparison to the classical method of chemical coagulation, which makes it a clean and eco-friendly technology (Zhu et al. 2005). The use of renewable energies to operate the electrocoagulation process emphasizes its character of green technology without impact over the climatic changes due to the electrical power from fossil resources (Rodriguez et al. 2007). Recently, Valero et al. (2008) demonstrated the reliability of using an electrocoagulation system supplied directly from a photovoltaic panel (Valero et al. 2008).

Even the recognized powerful method of electrochemical direct oxidation, that uses expensive anodes, such as platinum, boron-doped diamond, or ruthenium oxide coated titanium, seems to have low efficiencies in degrading this molecule (Zheng et al. 2012). Very recently, Khalfaoui et al. (2012) found that electro-Fenton process, which is an electrochemical indirect oxidation method, provides relatively good efficiency in terms of decolorization of R6G aqueous solutions. However, this technology is expensive and might be more appropriate as a final treatment stage before recycling in order to remove low-concentration pollutants.

Therefore, further studies must be performed in order to find a suitable cost-efficient treatment method for this kind of refractory and toxic compounds.

The electrochemical technology of electrocoagulation (EC) has captured a growing interest in the last few decades due to its cost-effective feature, especially in the treatment of wastewater containing refractory compounds (Akyol 2012; Holt et al. 2005; Mollah et al. 2001; Zaleschi et al. 2013). Likewise, this process results in high energy efficiency, cost-effectiveness, as well as low amounts of sludge (Chen 2004). Although, numerous contributions have been reported on the enhancement and optimization of this process, whereas the main stages involved in mechanisms of separating pollutants from

aqueous solutions by EC have been established only recently (Canizares et al. 2007; Chen 2004). The mechanism of electrocoagulation process is very complex, especially in the case of organic pollutants and is specific for each pollutant–electrode system. Nevertheless, several processes such as the in situ formation of the coagulation agent, adsorption, complexation, flotation, and/or precipitation are common to most of them (Zaleschi et al. 2012). In case of dyes, several main separation paths have been suggested by Daneshvar et al. (2006) as described by Eqs. (1)–(4):

Precipitation:

$$\text{Dye} + \text{monomeric M} => [\text{Dye}-\text{monomeric M}] \quad (1)$$

$$\text{Dye} + \text{polymeric M} => [\text{Dye}-\text{polymeric M}] \quad (2)$$

Adsorption:

$$\text{Dye} + \text{M(OH)n(s)} => [\text{sludge}] \quad (3)$$

$$[\text{Dye}-\text{polymeric M}](\text{s}) + \text{M(OH)n(s)} => [\text{sludge}] \quad (4)$$

The dye complexation with hydroxides generated into the solution or reduced by hydrogen is also possible. R6G dye molecule can be reduced before its adsorption onto the generated coagulant by the hydrogen gas produced in the electrochemical cell at the cathode (Sengil and Ozacar 2009).

A very recent study (Zheng et al. 2012) described the degradation mechanism of R6G dye by an electrooxidation process. It has been shown that the degradation of this dye occurs mainly through the direct oxidation by the anodic-generated active chlorine (hypochlorite ion, hypochlorous acid, or molecular chlorine) and hydroxyl radical. Since there are no studies reported on the mechanism of xanthene dyes by electrocoagulation process, this subject is addressed by the present research.

The main goal of the present work consists of the investigation of the removal of a xanthene dye from aqueous solutions by EC. The effects of several operating parameters such as current density, solution pH, electrolysis time, electrode configuration, and electrical current type were studied. The EC performances operated in batch regime were assessed in relation to removal efficiency and energy and material consumption. Fourier transform infrared spectroscopy, cyclic voltammetry, and chemical coagulation studies were undertaken in order to explain the decolorization mechanisms in addition to total organic carbon and UV–vis spectroscopy analyses.

2 Materials and Methods

2.1 Chemicals

Rhodamine 6G (99 %) was purchased from Sigma-Aldrich. Sodium chloride, sodium sulfate, hydrochloric acid, and sodium hydroxide were purchased from Lach-Ner, Neratovice, Czech Republic. $FeSO_4 \cdot 7H_2O$ (Merck, Germany) was used as coagulant in chemical coagulation tests. All chemicals were of analytical reagent grade and used without further purification.

R6G (Basic Red 1) with formula $C_{28}H_{31}N_2O_3Cl$ (Fig. 1) is a monocationic xanthene dye having the color index number 45160, a molecular weight of 479.02 g mol^{-1}, and the maximum absorbance corresponding to a wavelength of 530 nm.

The pH of treated solution was adjusted using H_2SO_4 or NaOH solutions.

2.2 Experimental Set-up

Electrocoagulation tests were carried out in a two-plan parallel electrode cell. The experimental set-up consists of an EC cell, a direct current (DC) power supply and a polarity changer, a magnetic stirrer, sensors connected to a multiparameter analyzer for measuring and recording the values of solution pH and conductivity, a data logger multimeter, and a computer for data recording. The experimental set-up was described in detail in our prior work (Secula et al. 2014).

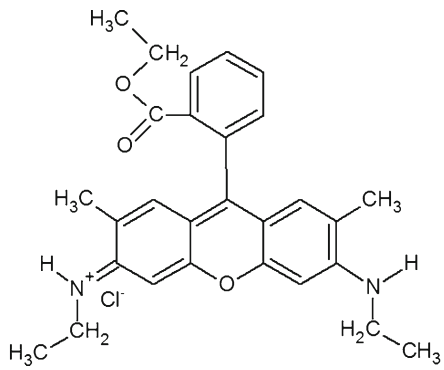

Fig. 1 Molecular structure of Rhodamine 6G

The manufactured electrodes with an effective electrode area of 183 cm^2 were positioned vertically and fixed at an interpolar distance of 4 mm. Aluminum or mild steel plate electrodes were used to investigate several electrode configurations (Al–Al, Fe–Al, and Fe–Fe).

The EC cell was operated in direct current and alternating pulse current modes. In the latter case, a polarity changer was employed in the electrical circuit between the electrodes and DC power supply (IT6322, 0-30V; 0-3A; ITECH, Nanjing, China). All the runs were performed at a room temperature of 25±0.5 °C.

The experiments were carried out in a batch mode. In each run, 1,000 cm^3 R6G model dye solution with different concentrations was placed into the EC cell and a gentle agitation was ensured along the EC test run to get a homogenous suspension by means of a BOECO MMS 3000 magnetic stirrer. The current density was set to a desired value and then the electrocoagulation was started. After drying, the electrodes were weighed before and after EC by using of an Acculab ATL-224-I analytical digital balance (accuracy 0.1 mg).

For each decolorization analysis, less than 5 cm^3 of aliquots were taken, let to settle for 1 h, centrifuged at 4,000 rpm by means of a BOECO S8 EBA20 centrifuge, and then spectrophotometrically analyzed.

A VC530 Voltcraft data logging multimeter connected to a PC was used to measure the cell voltage (sampling rate of signal, 1 value of voltage per second). Solution pH and conductivity were measured by means of a C863 Consort multiparameter analyzer, also connected to a PC.

The chemical coagulation experimental tests were performed by means of a Jar Test model JLT6, VELP Scientifica using $FeSO_4 \cdot 7H_2O$ as coagulant. In order to compare the EC removal efficiency in relation to R6G with that of the chemical coagulation process, similar coagulant doses were added in case of chemical coagulation and dosed electrically during the electrocoagulation process. Therefore, the coagulant doses used in chemical coagulation are equivalent to iron doses released into solution after 5, 15, 30, and 60 min of EC process.

The chemical coagulation was carried out initially at a fast stirring for 10 min (200 rpm), followed by gentle agitation for 20 min (20 rpm), and sedimentation for 30 min. Samples were taken from each jar and analyzed by UV–vis spectroscopy and total organic carbon (TOC).

2.3 Analytical Methods

The concentration of R6G was determined at λ_{max}= 530 nm by using a 5100 Hitachi UV/vis spectrophotometer. A distinct set of UV/VIS analyses were performed in order to determine the decolorization of some of the R6G dye aqueous solution in the presence of a chemical oxidant (sodium hypochlorite, 3 % active chlorine). A given volume of R6G dye solution (3.5 mL), C_i=20 mg/L, was mixed with a given amount of sodium hypochlorite (0.5 mL, 3 % NaOCl). After the solution homogenization, UV/VIS spectra were recorded until complete decolorization.

Sludge samples resulted by flotation, and sedimentation were collected, dried, and analyzed as such. Fourier transform infrared spectroscopy (FTIR) spectra of the resulted sludge by flotation and sedimentation were recorded in the range of 400–4,000 cm^{-1} by using a FTIR DIGILAB-FTS 2000 Spectrometer provided with an ATR (ZnSe) device, according to KBr pellet method.

The TOC was determined by a VCSN TOC analyzer using non-purgeable organic carbon (NPOC) and purgeable organic carbon (POC) methods.

The voltammetric studies were performed by using a VoltaLab 32 Electrochemical System Radiometer provided with data acquisition and processing VoltaMaster2 software. The electrolytic cell is provided with three electrodes, a platinum rotating disk electrode as working electrode (ø=2 mm), a saturated calomel electrode as reference electrode, and a platinum wire as auxiliary electrode.

2.4 Evaluation of EC Performance

The performance of EC technique was evaluated in terms of removal efficiency, energy, and electrode material consumptions.

The color removal efficiency (RE, %) was calculated using Eq. (5):

$$\mathrm{RE} = (C_0 - C) \cdot 100 / C_0 \quad (5)$$

where C_0 is the concentration of dye before EC (mg L^{-1}), and C is the concentration of dye after t min of EC (mg L^{-1}).

TOC removal efficiency (RE_{TOC}) was calculated with the following Eq. (6):

$$RE_{TOC} = (TOC_i - TOC_t) \cdot 100/TOC_i \quad (6)$$

where TOC_i is the total organic content before treatment (mg L^{-1}), and TOC_t is the total organic content after t min of treatment (mg L^{-1}).

Electrical energy consumption was determined in terms of unit energy demand (UED, kWh kg^{-1}), which is in fact the specific energy consumption (Secula et al. 2014) as follows:

$$UED = \left(I \cdot \int_0^t U \cdot dt \right) \Big/ \left(1,000 \cdot V \cdot C_i \cdot \frac{RE_t}{100} \right) \quad (7)$$

where U—cell voltage (V), I—current intensity (A), t—time (h), V—volume of treated solution (m^3), and RE_t—color removal efficiency at time t (%).

The amount of electrode material consumed can be calculated by means of Faraday's law and a correction factor (Secula et al. 2012).

$$UEMD_M = I \cdot t \cdot A/[f \cdot n \cdot F \cdot V \cdot C_i \cdot (RE_t/100)] \quad (8)$$

where $UEMD_M$—unit electrode material demand (kg/kg), t—time (s), n—number of electrons involved in oxidation/reduction reaction, F—Faraday's constant (C/mol), A—atomic mass of electrode material (g/mol), and f—ratio of electrochemical dissolution.

3 Results and Discussion

The effects of current density, initial pH, current type, electrode material and configuration, and EC time on the performances of EC of R6G dye solution are discussed in this section. The performance of EC is evaluated in terms of removal efficiency, specific energy, and electrode material consumption. Figure 2 shows the evolution of decolorization, TOC removal, and specific energy consumption during EC of R6G dye solution in a batch reactor corresponding to the experimental conditions described in the figure caption.

The EC process of R6G dye solution results in a relatively fast decolorization and after only 30 min, a value of 87.07 % is obtained for RE in relation to TOC.

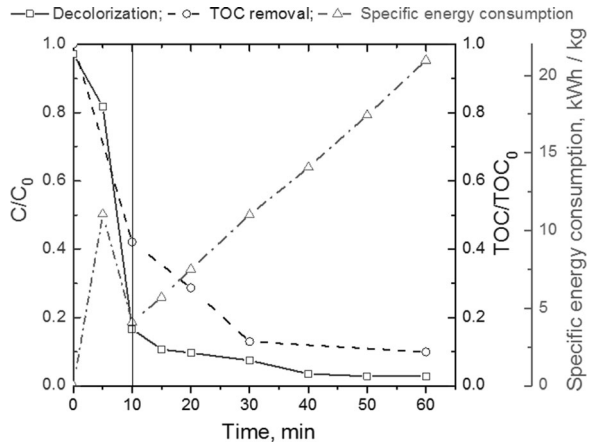

Fig. 2 Decolorization, TOC, and specific energy consumption evolution during EC process of a R6G dye aqueous solution. Experimental conditions: j=45 A/m^2, C_i=0.1 g/L, pH_i=5.37, and C_{NaCl}=1.5 g/L

However, the continuation of the EC process leads to marginal increases in RE, up to 97.29 % in relation to decolorization and 90.07 % in relation to TOC, respectively.

A minimal specific energy consumption of 4.1 kWh kg^{-1} of removed dye corresponding to a RE of 82.87 % (Fig. 2) is reached after 10 min of EC. Although, slightly higher values of dye removal efficiency are achieved when electrolysis time increases, the specific energy consumption increases significantly. Therefore, a cost-efficient operation of EC process requires the analysis.

3.1 Effect of Current Density

Experiments on the removal of R6G from synthetic solution with an initial dye concentration of 100 mg/L by EC were carried out at different current densities: 45, 65, 75; and 95 A/m^2, using iron electrodes with a surface of 183 cm^2 and 1.5 g/L NaCl supporting electrolyte. During the electrocoagulation process (60 min), samples were drawn from the cell for the determination of the concentration and the residual content in terms of TOC.

Based on the Faraday's law, when the densities of the current increased, the electro generated amount of the iron/aluminum ions also increased. In other words, as the applied current density is higher, more flocs will be formed and they will contribute to embed dye molecules, thus improving the removal/decolorization efficiency. At high current density, the coagulant amounts

and the gas bubbles density increase, thus helping the removal of molecules by flotation. When using iron anodes, the system generates Fe^{2+} ions from the dissolution of the sacrificial anode. These ions form oxyhydroxides, which are very good sorbents and coagulants and help to diminish the concentration of the organic compounds.

At a relatively short EC time, the current density has a strong effect on the aqueous solution color removal (Bayramoglu et al. 2007). At high current densities, the increased anodic dissolution leads to higher values of removal efficiency. Also, the production of gas bubbles increases while their size decreases, leading to the pollutant separation by flotation (Merzouk et al. 2010).

Figure 3 presents the evolution of removal efficiency of EC process applied to a 100-mg/L R6G solution at different values of current density.

Different behaviours regarding the assessment of the electrocoagulation performance for the synthetic solution of R6G removal efficiency were found, based on the electrochemical efficiency determination which was influenced by the current densities. Applying the current density of 95 A/m^2 allowed reaching the best results of the decolorization of R6G dye solutions. Thus, after 10 min of electrolysis, 87.97 % removal efficiency was achieved, and after 60 min of electrolysis, a removal efficiency of 99.68 % was reached. In comparison with other applied current densities (j=45 A/m^2→97.20 %; j=65 A/m^2→97.42 %; j=75 A/m^2→97.96 %), 95 A/m^2 is the most favorable current density in terms of the dye decolorization.

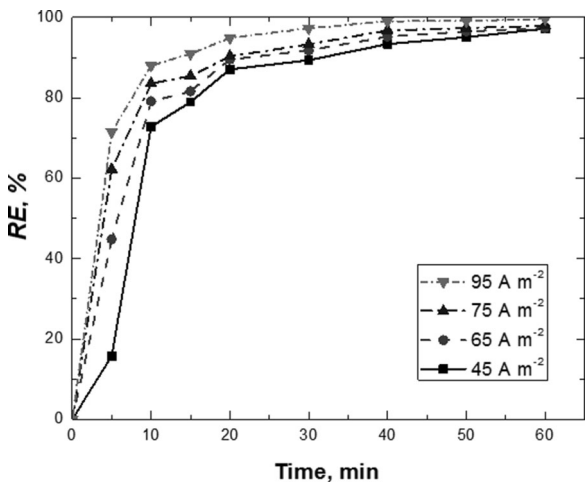

Fig. 3 Effect of the different current density on the evolution of R6G removal versus electrolysis time. Operating conditions: 100 mg/L R6G, 1.5 g/L NaCl, and pH_i=5.5; current density: *black square* 45 A/m^2, *black circle* 65 A/m^2, *black up-pointing triangle* 75 A/m^2, and *black down-pointing triangle* 95 A/m^2

However, the effect of current density should be also considered in terms of the removal efficiency and energy and electrode material consumptions.

Figure 4 describes the evolution of specific energy (Fig. 4a) and consumed electrode material (Fig. 4b) during EC process.

As the current density increases, both UED and $UEMD_{Fe}$ are higher. At the beginning of EC process, UED and $UEMD_{FE}$ are the highest for the case of the lowest value of the current density. This is an important observation concerning the mechanism of EC process. This non-proportionality between the specific consumptions over time shows that at the beginning, the main removal mechanism is not the adsorption of dye on the generated coagulant. We assume that especially at the beginning of the EC process, as long as the cathode surface is clean, cationic molecules of R6G may be trapped at the cathode surface and undergo reduction processes. Also, there is the possibility that at low pH values, i.e., at the beginning of the EC process, hydroxyl radicals are generated, which may further oxidize the molecule of dye (Ghernaout 2013).

Figure 5 shows the evolution of the solution pH during the EC process conducted in the already mentioned conditions.

In the case of the test performed at 45 A/m^2, the pH values are placed in the acid-neutral region for approximately 4 min at the beginning of the EC process, while at the other values of current density, the pH values increase quickly in less than 1 min after the process has started. This explains the sudden increase in the UED and $UEMD_{Fe}$ after 5 min. Hence, the deviation from the proportional increase of UED and $UEMD_{Fe}$ is explained by the important contribution of the degradation process of R6G.

3.2 Effect of the Initial pH

The performance of the EC process is usually influenced by the pH of the sample solution (Chen 2004). In order to establish the pH influence on the electrocoagulation process for dye removal by using iron electrodes, different values of the initial pH (3, 5.5, 7, and 9) were investigated.

Mollah et al. (2001) reported that the maximum efficiency of electrocoagulation process occurs at a pH

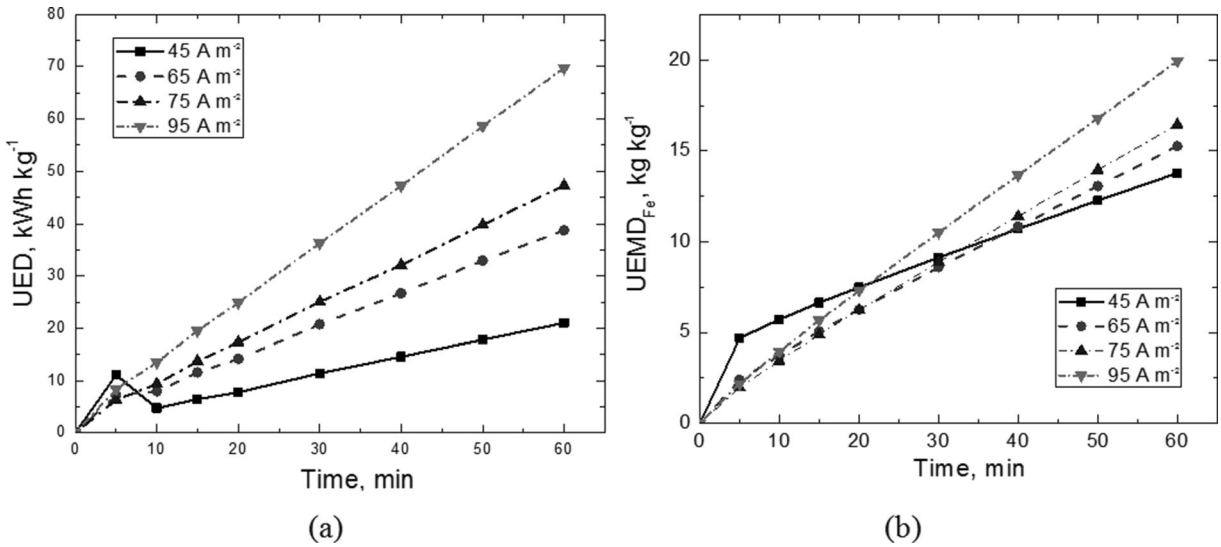

Fig. 4 Evolution of UED (**a**) and $UEMD_{Fe}$ (**b**) during EC process of 100 mg/L R6G solution (1.5 g/L NaCl, pH_i=5.5)

value of 6.9, which is considered the optimum pH for the most complex form of iron.

Figure 6 describes the evolution of removal efficiencies in relation to R6G removal and pH values, respectively, during the EC process conducted at the highest current density from the considered range.

The plots in Fig. 6a indicate that the removal efficiencies increase with the initial pH values. The curves in Fig. 6b show that the test at an initial pH of 3 reaches a neutral pH value in only 3 min, a pH value of 8 in 20 min, and at the end of the process, the treated solution has a pH value of 8.2. For the tests conducted at initial pH values of 5.5, 7, and 9, respectively, the solution pH increases in less than 5 min above 9 and stabilizes at 9.5, 9.8, and 10, respectively.

At high values of current density, the generation of hydroxyl ions at the cathode leads to this fast increase in solution pH, which makes the pH parameter to be of less importance toward the EC performance.

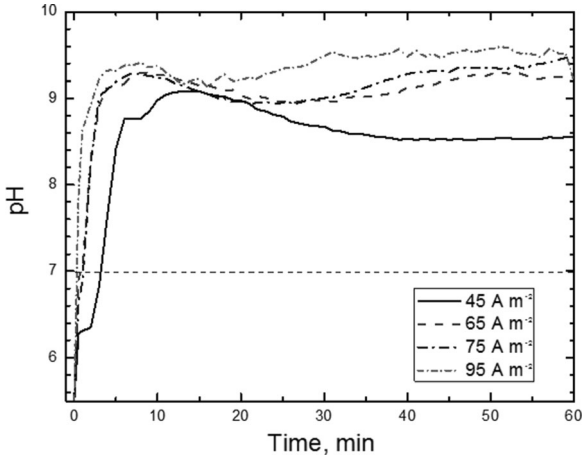

Fig. 5 The evolution of pH during EC process conducted at different values of current densities (100 mg/L R6G, 1.5 g/L NaCl, pH_i=5.5)

3.3 Effects of the Electrode Material and Current Type

Different metal pairs of electrodes (Fe–Fe, Al–Al, and Fe–Al) were used in order to study the influence of the electrode material on the performance of EC in terms of removal efficiency, specific energy, and electrode material consumptions. Figure 7 presents the performance of EC process operated with different electrode configurations and types of current (direct current (DC) and alternative pulsed current (APC)). In order to emphasize the effects of electrode material and current type, several test were conducted at a relatively high value of current density, 109 A/m^2, and a high concentration of dye, 1 g/L. The initial pH of dye solution was of 5.5, and the concentration of supporting electrolyte was of 1.5 g/L.

In terms of removal efficiency, the highest values are obtained for iron-pair configuration operated in APC and DC mode and Fe–Al operated in DC mode. On the other hand, aluminum-based configurations are not effective in removing this dye from aqueous solution. This was mainly observed in the experimental tests,

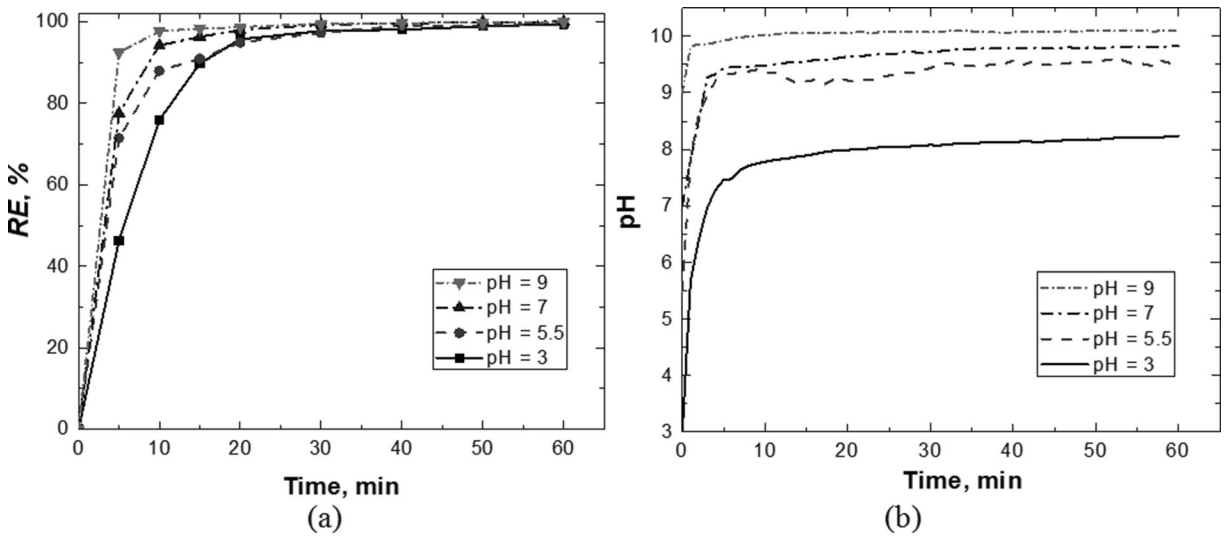

Fig. 6 The evolution of removal efficiency (**a**) and pH (**b**) during EC process conducted at different values of current densities (100 mg/L R6G; 1.5 g/L NaCl: pH_i=5.5: current density, 95 A/m^2)

when iron-pair configuration leads to the separation of dye by either flotation or sedimentation, while in the case of Fe–Al configuration operated in DC mode, a spongious layer was formed on the cathode surface. Actually, R6G is a basic dye and migrates towards the cathode electrode, where it is trapped, especially when both ferric and aluminum ions are present in the solution. It was also noticed that the use of APC mode avoids the formation of the spongious layer and the removal efficiency decreases substantially.

The Fe–Fe electrode pair operated in APC mode leads to the fastest removal of R6G, when 98 % of dye is removed in only 30 min of EC process. This emphasizes the positive influence of the APC mode in comparison with the more common DC operation of EC process.

Concerning the specific energy consumption, i.e., electric energy consumed per unit of dye removed, the most effective electrode configuration is that based on iron electrodes. Independently of the EC time, this configuration provides the lowest values of UED, which means high removal efficiency in relation to R6G with low energy consumption. In the case of this electrode configuration, the APC mode proves also to be more economical than DC mode for the operation of EC process. Thus, an UED of 6.84 kWh kg^{-1} is obtained in case of EC process based on Fe–Fe electrode configuration operated in APC mode. Due to the fact that UED is proportional to the amount of dye removed, it is expected that this indicator will evolve in a contrary direction to that of the removal efficiency. However, Fe–Al configuration operated in DC mode seems to behave differently mostly due to the formation of the spongious layer on the electrode. Operating in galvanostatic regime, the voltage of the EC cell increases (i.e., constant current intensity), resulting in higher electric energy consumption, more obvious after 2 h of EC processing.

Since the electrode material consumption is directly proportionally with the current applied, it is expected that Fe–Fe electrode configuration will provide also the lowest values of $UEMD_M$. However, it should be taken into account that the anodic dissolution of iron requires the transfer of only two electrons (Fe^{2+}), while in case of aluminum, three electrons are donated (Al^{3+}). This means that for a similar amount of electrical energy, a higher amount of iron is dissolved than in the case of aluminum. Nevertheless, as Eq. (3) defines the chemical dissolution of metal is also taken into account and for this electrode pair, the aluminum chemically dissolves, while the amount of dissolved iron is very close to that predicted by Faraday's law. Figure 7c shows that the lowest values of the specific electrode material consumption are obtained with Fe–Fe electrode configuration operated in APC mode for only 30 min, when a removal efficiency of 98 % is achieved, which corresponds to a $UEMD_{Fe}$ (iron-based configuration) of 1.73 kg of iron per kilogram of dye removed. If the process continues furthermore, the

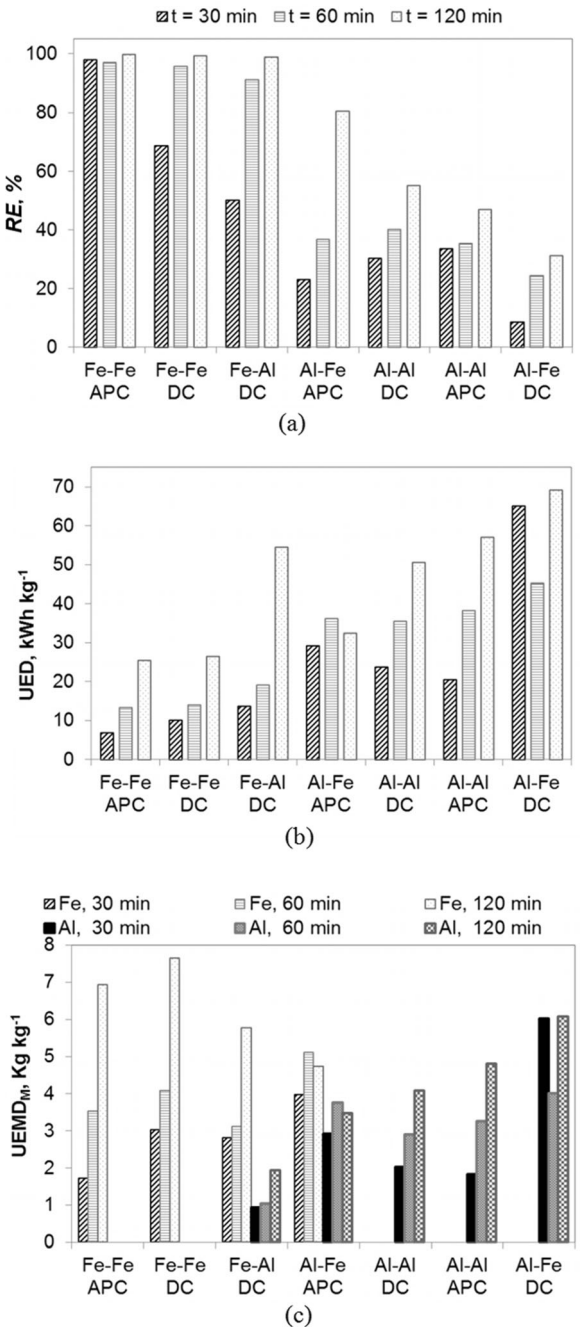

Fig. 7 Effect of electrode configuration and current type on the performance of EC process (removal efficiency (**a**), UED (**b**), and $UEMD_M$ (**c**)) for R6G dye removal at different times (j=109 A/m^2, C_{iR6G}=1 g/L, C_{NaCl}=1.5 g/L, pH_i=5.5)

specific electrode material consumption doubles after 1 h of EC, while after 2 h, it increases four times. Therefore, the operation time is a critical parameter for this process.

3.4 Mechanism of Rhodamine 6G Separation by EC

3.4.1 Voltammetry Analysis

In order to establish the removal mechanism of R6G, it might be of interest to establish whether direct oxidation plays an important role in the degradation of R6G processes occurring in an electrolytic cell. Thus, the cyclic voltammograms of several R6G dye solutions using NaCl as support electrolyte were recorded.

Figure 8a, b presents the cyclic voltammograms obtained for aluminum and iron electrode, respectively, in the presence of (1) 0.025 M NaCl, (2) 20 mg/L+ 0.0256 M NaCl, and (3) 100 mg/L R6G+0.0256 M NaCl, respectively, recorded in the potential range from −0.3 to 1.25 V/SCE, in the case of iron, and −0.7÷ 1.25 V/SCE, in the case of aluminum, at a scan rate of 0.05 V/s.

The cyclic voltammograms recorded in the potential ranges located just before the potential of chlorine evolution present no anodic peak. This means that no direct electrooxidation of R6G at the electrode surface occurred besides the electrocoagulation process. The dissolution of the working electrode takes place at lower values of current in the case of iron-based material compared to aluminum. The presence of the R6G dye into the electrochemical systems leads to a decrease in current density value, which means that the electrodes get passivated.

3.4.2 UV–VIS Analysis

The UV–VIS spectra of R6G dye solution and those treated either with sodium hypochlorite or by electrocoagulation were recorded and compared. Figure 9 presents the UV–VIS spectra of 20 mg/L R6G aqueous dye solution (Fig. 9, line (1)), dye solution treated by NaOCl for 1 min (Fig. 9, line (2)) and for 60 min (Fig. 9, line (3)), and dye solution treated by EC process (Fig. 9, line (4)).

In the case of sodium hypochlorite treatment, the peak specific to hypochlorite ion appears at λ=290 nm. The peak corresponding to the chromophore groups of R6G disappears completely and the residual value of hypochlorite peak decreases slightly. After 1 min of oxidation with 3 % sodium hypochlorite, the initial dye concentration of 20 mg/L decreases 5 mg/L R6G dye.

Based on the recorded UV–VIS spectra of the treated synthetic R6G dye, it can be concluded that the

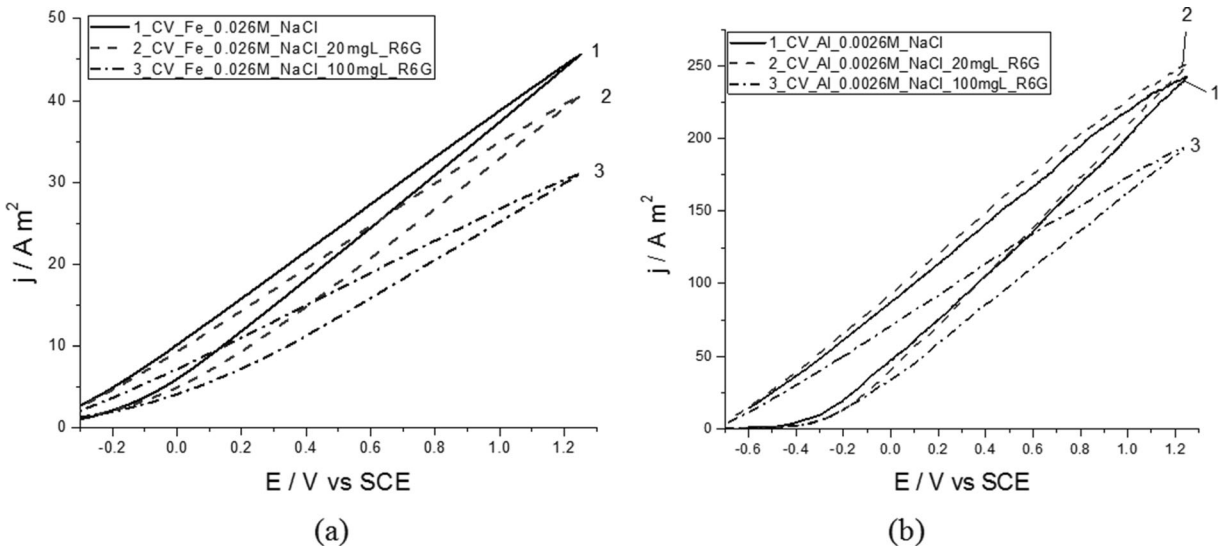

Fig. 8 Cyclic voltammograms for iron (**a**) and aluminum electrode (**b**), respectively, in the presence of *(1)* 0.0256 M NaCl, *(2)* 20 mg/L+ 0.0256 M NaCl, and *(3)* 100 mg/L R6G+0.0256 M NaCl

chromophore group is destroyed by the oxidation process. Thus, due to the fact that the concentration of dye decreases, the aqueous solution becomes colorless.

Hypochlorite ions form constantly from NaCl during the electrocoagulation process. If the electrocoagulation process mechanism would have been based on the oxidation process, it could be expected to have a hypochlorite ion peak as the dye concentration decreased. The process was favored by the relatively strong alkaline pH of the treated solution.

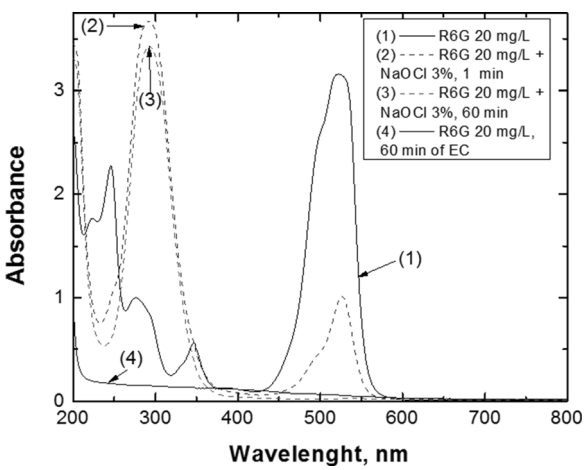

Fig. 9 UV–vis spectra of *(1)* initial R6G solution, *(2)* R6G solution treated by EC (j=95 A/m^2; C_i=20, 50, and 100 mg/L, pHi=7; C_{NaCl}=1.5 g/L, iron electrodes), and R6G solution treated with NaClO after *(3)* 1 min and *(4)* 60 min, respectively

Line (4) in Fig. 9 shows however that hypochlorite ion is not present in the solution treated by EC; its formation is relatively marginal. Therefore, the removal mechanism of R6G from aqueous solutions is EC cannot be assigned to the oxidation of dye by means of hypochlorite ion in the bulk solution.

The efficiency of the chemical coagulation was also studied. However, extremely low values were obtained for the removal efficiency (approximately, 1–3 %). This proves that the separation process by means of ferric hydroxide in the EC process is also of low importance.

3.4.3 FTIR Analysis

The aim of the IR spectroscopy study was to establish the mechanisms that contribute to decolorization of aqueous solutions containing R6G by electrocoagulation process starting from the reactions occurring at the anode, cathode, and in the bulk solution.

R6G molecule is slightly soluble in water due to its polar molecular structure. During the electrocoagulation process, the R6G molecules become nonpolar, insoluble, and an orange/red foam is produced, depending on the dye concentration. In order to elucidate this phenomenon and determine the mechanism of foam formation, the IR spectra of the commercial dye, foam, and sludge which resulted after electrocoagulation process were recorded and compared. Figure 10 shows the recorded spectra.

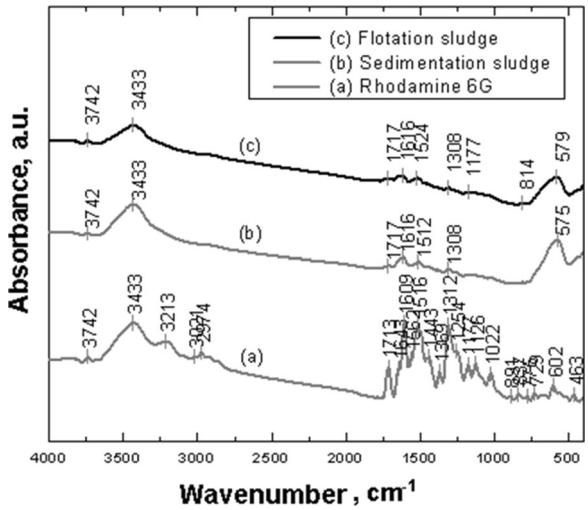

Fig. 10 Rhodamine 6G (*a*), flotation (*b*), and sedimentation (*c*) sludge FTIR spectra

Thus, in order to determine the foam formation mechanism, FTIR analysis was performed. It can be observed that the secondary aromatic amino group peak (3,213, 3,021 cm^{-1}) increases in intensity for the foam case as compared to the R6G peak. This phenomenon is attributed to the secondary amino group detachment (Table 1 presents the characteristic groups IR frequencies of R6G dye as determined by the FTIR analysis).

The peaks corresponding to the foam at 1,312 cm^{-1} and 1,713 cm^{-1}, respectively, in R6G spectra are specific to the aryl esters (C-O-C, C=O) and in the foam spectrum, the intensity of these peaks is increasing. The peak from 1,516 cm^{-1} corresponds to secondary amino aromatic group. As compared to the peak recorded in R6G spectra, the lower intensity of this peak in foam spectra is due to amino group detachment. In the range of 3,500–3,100 cm^{-1}, a wide band of medium frequency corresponding to the vibration groups N–H and O–H appears (Bakkialakshmi and Menaka 2010; Liu et al. 1998; Moamen et al. 2011; Nieckarz et al. 2013). The bands with the peaks at 3,213 cm^{-1} and 3,021 cm^{-1} are assigned to the valence vibrations specific to N–H group in the IR spectrum of R6G. In the spectra of the sedimentation and flotation sludge, these bands are not present, proving that the decolorization of the treated aqueous solutions is due to the destruction of N–H groups. The band of average intensity due to elongation vibration of methyl group ($-CH_3$) occurs in the R6G spectrum at 2,974 cm^{-1}, and the band due to the vibration of symmetric deformation occurs at 1,369 cm^{-1}. The IR data of the sludge show that the groups of the N–H and $–CH_3$ disappear. The decolorization of R6G dye solutions is explained by the destruction of N–H and $–CH_3$ groups, which are detached from the dye molecule.

The main mechanism of EC may be attributed to the dye deamination and demethylation by redox processes. Thus, it is very likely that the cationic molecule of R6G may undergo a reduction process at the cathode surface. Some authors consider also the possibility that hydroxyl radicals are generated in the EC process, especially at low values of pH (Ghernaout 2013), which may further oxidize the molecule of dye. This mechanism is supported by FTIR analysis as well as by the experimental observations. At the end of EC process, the cathode is covered with a layer of foam, where dye molecules and the side products are trapped.

The mechanism of electrocoagulation process is rather complex. The IR spectroscopy analysis showed that the dye molecule is involved in redox processes taking place in the vicinity of the electrode surface, resulting in its deamination and demethylation. After deamination and demethylation, the polar molecules become nonpolar and insoluble and easier to separate. This mechanism is supported by our experimental tests performed at different inter-electrode distance. The value of removal efficiencies decrease with the inter-electrode distances. This means that the dye molecule is more difficult to separate in its polar form.

Scheme 1 presents a conceptual model proposed for the electrocoagulation of an aqueous solution containing R6G in order to illustrate the mechanism of decolorization.

Table 1 Characteristic groups IR frequencies of R6G dye

Group name	Group	R6G IR (cm^{-1})	Foam IR (cm^{-1})	Sludge IR (cm^{-1})
Aryl-ester	C-O-C	1,312	1,308	1,308
Carbonyl	C=O	1,713	1,717	1,717
Amino	N–H	3,213, 3,021	–	–
Methyl	$-CH_3$	2,974, 1,369	–	–

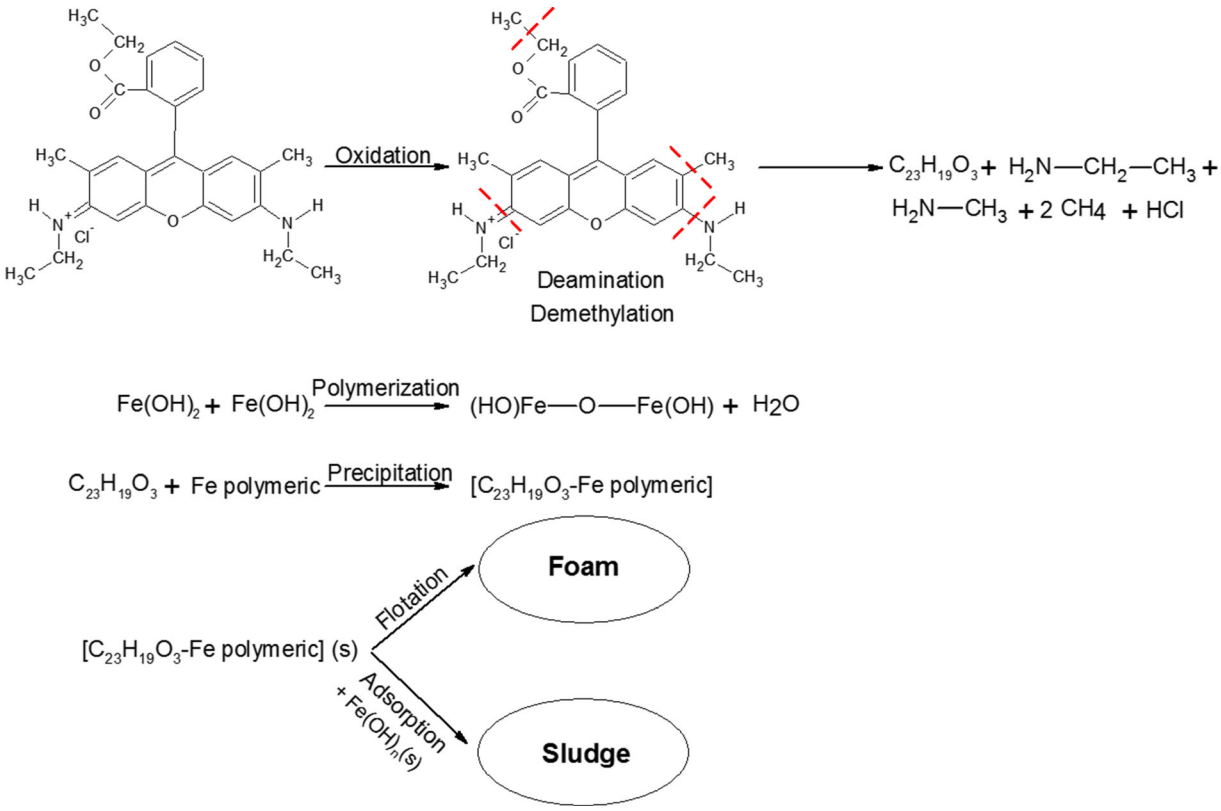

Scheme 1 Schematic diagram of the aqueous solution containing R6G

The main reactions are the anodic dissolution of iron electrode in iron ions in solution and the formation of iron hydroxide by the reaction with hydroxyl ions generated at the cathode in the bulk solution. As the concentration of ferrous hydroxide increases, the polymerization reaction takes place, resulting in polymeric iron flocs, which may precipitate the phenyl-xanthene radicals remained in the bulk solution after the demethylation and deamination processes. Furthermore, the flocs are separated by flotation with the support of the molecular hydrogen generated at the cathode (especially at relatively high values of current density),or by sedimentation.

4 Conclusions

This paper presents a study concerning the assessment of operational parameters on the removal of R6G (a xanthene dye) by electrocoagulation operated in batch and galvanostatic regime.

The effects of several operating parameters such as pH, current density, initial dye concentration, electrolysis time, electrode configuration (Fe–Fe, Al–Al, and Fe–Al), and electrical current type on the EC performances were studied.

The best performance of EC process was obtained at a current density of 95 A/m^2, pH value of 9, using iron electrode configuration. Under these conditions, the EC of a 100-mg/L dye R6G aqueous solution leads to 100 % decolorization; after 60 min, the removal efficiency in relation to TOC reaches the highest value of 82.98 %. The optimal electrocoagulation time is 5 min, when 92.4 % decolorization removal efficiency is reached with a specific energy consumption of 6.31 kWh kg^{-1}.

It has been noticed that the Fe–Fe, electrode configuration operated in APC regime provided the best dye solution decolorization rate.

The mechanism of the R6G removal by EC was also discussed. It was found that polymeric iron flocs co-precipitate with the phenyl-xanthene radicals remained in the bulk solution after the demethylation and deamination processes. The formed flocs are easily separated by flotation or sedimentation.

References

Akyol, A. (2012). Treatment of paint manufacturing wastewater by electrocoagulation. *Desalination, 285*, 91–99.

Ansari, A. T., Sundaramoorthy, N., & Kavitha, M. (2011). Adsorption, bisorption and discolourisation of rhodamine-B and basic violet- 2 using fungi isolated form soil samples collected near textile dye industry. *International Journal of Research in Pharmaceutical and Biomedical Sciences, 2*(4), 1706–1710.

Aquino, J. M., Rocha-Filho, R. C., Rodrigo, M. A., Saez, C., & Canizares, P. (2013). Electrochemical degradation of the reactive 141 dye using a boron-doped diamond anode. *Water, Air, and Soil Pollution, 224*, 1397–1399.

Babu, B. R., Parande, A. K., Raghu, S., & Kumar, T. P. (2007). Textile technology cotton textile processing: waste generation and effluent treatment. *Journal of Cotton Science, 11*, 141–153.

Bakkialakshmi, S., & Menaka, T. (2010). A detailed spectroscopic study on the interaction of Rhodamine 6G with two amines. *International Journal of Current Research, 10*, 21–24.

Bayramoglu, M., Eyvaz, M., & Kobya, M. (2007). Treatment of the textile wastewater by electrocoagulation: economic evaluation. *Chemical Engineering Journal, 128*, 155–161.

Bayramoglu, G., Adiguzel, N., Ersoy, G., Yilmaz, M., & Arica, M. Y. (2013). Removal of textile dyes from aqueous solution using amine- modified plant biomass of *A. caricum*: equilibrium and kinetic studies. *Water, Air, and Soil Pollution, 224*, 1640–1647.

Bebeselea, A., Manea, F., Radovan, C., Burtica, G., Teodosiu, C., Pop, A., Proca, C., & Corb, I. (2008). The degradation of phenol derivates from wastewaters by electrochemical treatment. *WIT Transactions on Ecology and the Environment, 111*, 435–444.

Căilean, D., & Teodosiu, C. (2012). Integrated ultrasonication-ultrafiltration process for the treatment of textile effluents: assessment of operational parameters. *Environmental Engineering and Management Journal, 11*(2), 259–270.

Căilean, D., Teodosiu, C., & Brînză, F. (2009). Studies regarding advanced processes used for reactive dyes removal from textile effluents. *Environmental Engineering and Management Journal, 8*(5), 1045–1051.

Căilean, D., Teodosiu, C., & Ungureanu, F. (2013). Engineering challenges in advanced wastewater treatment. *Environmental Engineering and Management Journal, 12*(8), 1541–1551.

Canizares, P., Jimenez, C., Martinez, F., Saez, C., & Rodrigo, M. A. (2007). Study of the electro-coagulation process using aluminium and iron electrodes. *Industrial & Engineering Chemistry Research, 46*, 6189–6195.

Chen, G. (2004). Electrochemical technologies in wastewater treatment. *Separation and Purification Technology, 38*, 11–41.

Daneshvar, N., Oladegaragoze, A., & Djafarzadeh, N. (2006). Decolorization of basic dye solutions by electrocoagulation: an investigation of the effect of operational parameters. *Journal of Hazardous Materials, 129*, 116–122.

Ghernaout, D. (2013). Advanced oxidation phenomena in electrocoagulation process: a myth or a reality? *Desalination and Water Treatment*. doi:10.1080/19443994.2013.792520.

Halterman, R. L., Moore, J. L., Yakshe, K. A., Halterman, J. A. I., & Woodson, A. (2010). Inclusion complexes of cationic xanthene dyes in cucurbituril. *Journal of Inclusion Phenomena and Macrocyclic Chemistry, 66*, 231–241.

Holt, P. K., Barton, G. W., & Mitchell, C. A. (2005). The future for electrocoagulation as a localised water treatment technology. *Chemosphere, 59*, 355–367.

Ingale, S. V., Wagh, P. B., Tripathi, A. K., Srivastav, R., Singh, I. K., Bindal, R. C., & Gupta, S. C. (2012). TiO_2—polysulfone beads for use in photo oxidation of rhodamine B. *Soft Nanoscience Letters, 2*, 67–70.

Jekel, M. (1997). Wastewater treatment in the textile industry, in: Treatment of wastewaters from textile processing, *TU-Berlin SchiftenreihebiologischeAbwasserreinigung*, Vol. 9, Berlin, Germany.

Jhonsi, M. A., Kathiravan, A., & Renganathan, R. (2009). Photoinduced interaction between xanthene dyes and colloidal CdS nanoparticles. *Journal of Molecular Structure, 921*, 279–284.

Khalfaoui, N., Boutoumi, H., Khalaf, H., Oturan, N., & Oturan, M. A. (2012). Electrochemical oxidation of the xanthene dye rhodamine 6g by electrochemical advanced oxidation using Pt and BDD anodes. *Current Organic Chemistry, 16*, 2083–2090.

Khan, T. A., Sharma, S., & Ali, I. (2011). Adsorption of Rhodamine B dye from aqueous solution onto acid activated mango (Magniferaindica) leaf powder: equilibrium, kinetic and thermodynamic studies. *Journal of Toxicology and Environmental Health Sciences, 3*(10), 286–297.

Liu, C. M., Xiong, R. G., You, X. Z., & Chen, W. (1998). Crystal Structure and luminiscence spectra of transition metal complexes of Rhodamine 6G:$R_2[CuCl_4]$ $3H_2O$ and $R_2[MnCl_4]$ $(EtOH)_{1/2}$ [R = 9-(2-ethoxycarbonyl)phenyl-3,6-bis(ethylamino)-2,7-dimethylxanthylium. *Acta Chimica Scandinavica, 52*, 883–890.

Martinez-Huitle, A. C., & Brillas, E. (2009). Decontamination of wastewaters containing synthetic organic dyes by electrochemical methods: a general review. *Applied Catalysis B: Environmental, 87*, 105–145.

Merzouk, B., Madani, K., & Sekki, A. (2010). Using electrocoagulation–electroflotation technology to treat synthetic solution and textile wastewater, two case studies. *Desalination, 250*(5), 573–577.

Merzouk, B., Gourich, B., Madani, K., Vial, C., & Sekki, A. (2011). Removal of a disperse red dye from synthetic wastewater by chemical coagulation and continuous electrocoagulation.a comparative study. *Desalination, 272*, 246–253.

Moamen, S. R., Hamada, M. A., Killa, M. Y., & El-Sayed. (2011). IR 1H-NMR, UV–vis and thermal studies on the Rhodamine 6G chargetransfer complexes. *Bulletin of the Chemical Society of Ethiopia, 25*(1), 137–146.

Mollah, M. Y. A., Schennach, R., Parga, J. R., & Cocke, D. L. (2001). Electrocoagulation (EC)—science and applications. *Journal of Hazardous Materials, 84*, 29–41.

Nieckarz, E. J., Jos, O., Giel, B., Pavel, S., & Renato, Z. (2013). Infrared multiple photon dissociation (IRMPD) spectroscopy of oxazine dyes. *Physical Chemistry Chemical Physics, 15*, 5049.

Parsa, J. B., Vahidian, H. R., Soleymani, A. R., & Abbasi, M. (2011). Removal of Acid Brown 14 in aqueous media by electrocoagulation: optimization parameters and minimizing of energy consumption. *Desalination, 278*, 295–302.

Rodriguez, J., Stopic, S., Krause, G., & Friedrich, B. (2007). Feasibility assessment of electrocoagulation towards a new sustainable wastewater treatment. *Environmental Science & Pollution Research, 14*(7), 477–482.

Secula, M. S., Cretescu, I., & Petrescu, S. (2011). An experimental study of indigo carmine removal from aqueous solution by electrocoagulation. *Desalination, 277*(1–3), 227–235.

Secula, M. S., Cretescu, I., & Petrescu, S. (2012). Electrocoagulation treatment of sulfide wastewater in a batch reactor: effect of electrode material on electrical operating costs. *Environmental Engineering and Management Journal, 11*, 1485–1491.

Secula, M. S., Zaleschi, L., Stan, C. S., & Mamaliga, I. (2014). Effects of electric current type and electrode configuration on the removal of Indigo Carmine from aqueous solutions by electrocoagulation in a batch reactor. *Desalination and Water Treatment*. doi:10.1080/19443994.2013.811116.

Sengil, A., & Ozacar, M. (2009). The decolorization of C.I. reactive black 5 in aqueous solution by electrocoagulation using sacrificial iron electrodes. *Journal of Hazardous Materials, 161*, 1369–1376.

Tang, S. K., Teng, T. T., Alkarkhi, A. F. M., & Li, Z. (2012). Sonocatalytic degradation of rhodamine B in aqueous solution in the presence of TiO2 coated activated carbon. *International Journal of Environmental Science and Development, 3*(1), 110–115.

Tiwari, R., Ameta, S. C., & Sharma, M. K. (2011). Effect of photocatalytic treatment on quality parameters of Rhodamine B. *Journal of Environmental Research and Development, 6*(1), 82–85.

Valero, D., Ortiz, J. M., Expósito, E., Montiel, V., & Aldaz, A. (2008). Electrocoagulation of a synthetic textile effluent powered by photovoltaic energy without batteries: direct connection behaviour. *Solar Energy Materials and Solar Cells, 92*(3), 291–297.

Venkatraman, B. R., Gayathri, U., Elavarasi, S., & Arivoli, S. (2012). Removal of Rhodamine B dye from aqueous solution using the acid activated cynodondactylon carbon. *Der Chemica Sinica, 3*(1), 99–113.

Vlaicu, A., Vlaicu, I., Pop, A., Manea, F., & Radovan, C. (2011). Degradation of humic acid from water by advanced electrochemical oxidation method. *Water Science and Technology: Water Supply, 11*(1), 85–95.

Wei, M. C., Wang, K. S., Huang, C. L., Chiang, C. W., Chang, T. J., Lee, S. S., & Chang, S. H. (2012). Improvement of textile dye removal by electrocoagulation with low-cost steel wool cathode reactor. *Chemical Engineering Journal, 192*, 37–44.

Xia, Y., Yin, D., Shi, M., Yao, Y., Huang, W., & Li, Z. (2012). Preparation of Ag2SO3 based composites and their efficient degradation of Rhodamine B under visible light irradiation. *Materials Letters, 87*, 58–61.

Zaleschi, L., Teodosiu, C., Cretescu, I., & Rodrigo, M. A. (2012). A comparative study of electrocoagulation and chemical coagulation processes applied for wastewater treatment. *Environmental Engineering and Management Journal, 11*(8), 1517–1525.

Zaleschi, L., Sáez, C., Cañizares, P., Cretescu, I., & Rodrigo, M. A. (2013). Electrochemical coagulation of treated wastewaters for reuse. *Desalination and Water Treatment, 51*(16–18), 3381–3388.

Zheng, Y. M., Yunus, R. F., Nanayakkara, K. G. N., & Chen, J. P. (2012). Electrochemical decoloration of synthetic wastewater containing rhodamine 6G: behaviors and mechanism. *Industrial and Engineering Chemistry Research, 51*, 5953–5960.

Zhu, B., Clifford, D. A., & Chellam, S. (2005). Comparison of electrocoagulation and chemical coagulation pretreatment for enhanced virus removal using microfiltration membranes. *Water Research, 39*, 3098–3108.

Zollinger, H. (2003). *Color chemistry: syntheses, properties, and applications of organic dyes and pigments*. Switzerland: Wiley.